RSC Advances

PAPER

View Article Online
View Journal | View Issue

Cite this: *RSC Adv.*, 2021, **11**, 14710

Synthesis of alkyl polyglycosides using SO_3H-functionalized ionic liquids as catalysts†

Wenliang Wu,[ab] Hongshuai Gao, *[ab] Bin Hai,[b] Binqi Wang,[b] Min Yu[b] and Yi Nie *[ab]

An effective process for synthesis of alkyl polyglycosides (APG) was developed using SO_3H-functionalized ionic liquids (SFILs) as catalysts. Four SFILs, [PSmim][HSO_4], [PSmim][*p*TSA], [PSPy][HSO_4] and [PSPy][*p*TSA], were designed and synthesized for APG synthesis. The results indicated that [PSmim][HSO_4] shows the best catalytic performance among these four SFILs, which has a great agreement with the order of their acidities. When the [PSmim][HSO_4] was used as catalyst, the reaction time could be decreased from 24 h to 8 h, and molar ration of *n*-octanol to glucose could be decreased from 5 : 1 to 3 : 1 under the optimization reaction conditions. In addition, the [PSmim][HSO_4] could be easily regenerated and recycled at least 5 times with slight decrease in catalytic activity. Moreover, the catalytic mechanism of [PSmim][HSO_4] was further investigated by molecular simulation. The high catalytic activity of [PSmim][HSO_4] is attributed to hydrogen bonds between [PSmim][HSO_4] and glucose and *n*-octanol, which could accelerate the protonation of glucose and removal of hydrogen ions from the hydroxyl in *n*-octanol.

Received 14th January 2021
Accepted 8th April 2021

DOI: 10.1039/d1ra00337b

rsc.li/rsc-advances

1 Introduction

Alkyl polyglycosides (APG), produced from glucose and fatty alcohols, are one kind of renewable green non-ionic surfactants. Because of good surfactant properties and complete biodegradability, they have been applied in many fields, such as the detergent, cosmetic, and pharmaceutical cleaning industries.[1–3] At present, the synthesis of APG is usually *via* Fischer's glucosylation as shown in Fig. 1. Depending on the type of carbohydrate used, all manufacturing processes for the Fischer synthesis of APG could be attributed to two approaches, namely the direct glucosylation synthesis process[2] and the transacetalization process.[4,5] The direct glucosylation synthesis has the features of a short synthesis path, low energy consumption, easy operation and being cost-effective, and is more suitable for industrial production than the transacetalization process.[1,6] For the current production technology of commercial APG, mineral acids such as concentrated sulfuric acid are usually chosen as catalysts, but they are non-recyclable and environmentally incompatible.[7–10] To overcome the drawbacks of the traditional catalyst, the development of a green catalyst reaction system for direct glucosylation synthesis has attracted much attention in the past few years.[11] Ludot *et al.*[5] developed an efficient method using sulfoxides and sulfones as solvent for the synthesis of APG without catalyst. Although the conversion rate of xylose for APG produced from xylose and decanol could be up to 83%, the reaction temperature is up to 423.15 K. Augé *et al.*[6] established a new method for the synthesis APG using the metal triflate as catalyst and 1-butyl-3-methylimidazolium trifluoromethanesulfonate as solvent. The high conversion rate (74%) of glucose produced from glucose and *n*-octanol could be obtained when the temperature is 353.15 K, but the reaction time need to be extended up to 24 h. Therefore, the development of novel effective catalyst for synthesis of APG is highly desired.

In recent years, the applications of room temperature ionic liquids (RTILs) as "green" solvents or catalysts for organic synthesis have been extensively investigated owing to their negligible volatility, excellent thermal stability, remarkable solubility and the variety of structures available.[12–16] In addition, the design of acidic ILs to replace traditional mineral acids in chemical processes have been paid much attention by researchers.[17–19] It was found that the acidities of these ILs were enhanced with the presence of SO_3H groups. These ILs displayed excellent catalytic performances as homogeneous catalysts in many typical acid-catalyzed organic reaction.[20–23] For

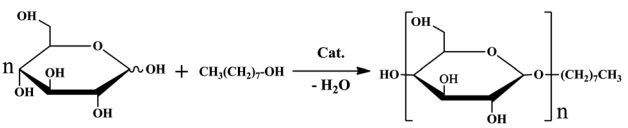

Fig. 1 Schematic illustration of Fischer's glycosylation.

[a]*Beijing Key Laboratory of Ionic Liquids Clean Process, CAS Key Laboratory of Green Process and Engineering, State Key Laboratory of Multiphase Complex System, Institute of Process Engineering, Chinese Academy of Sciences, 100190, Beijing, China. E-mail: hsgao@ipe.ac.cn; ynie@ipe.ac.cn; Fax: +86-10-82544875; Tel: +86-10-82544875*

[b]*Zhengzhou Institute of Emerging Industrial Technology, 450046, Zhengzhou, China*

† Electronic supplementary information (ESI) available: The ^{1}H NMR, FTIR, ESI-MS and decomposition temperature data of four SFILs are presented. See DOI: 10.1039/d1ra00337b

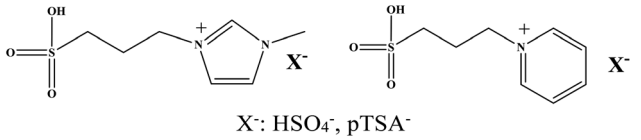

X^-: HSO_4^-, $pTSA^-$

Fig. 2 Structures of four SO_3H-functionalized ILs.

example, SO_3H-functionalized ILs (SFILs) show the excellent catalytic activity as catalysts in synthesis of furylmethane derivatives.[22] However, their application in the direct glucosylation synthesis has not been reported. Therefore, we hope to make use of the advantages of SFILs to improve the efficiency of APG synthesis, simplify the production process, and investigate the reaction mechanism in depth. In this work, four SO_3H-functionalized ILs were synthesized for direct glucosylation synthesis as catalysts and the structures of the SFILs are shown in Fig. 2. The effect of experimental conditions such as reaction temperature, reaction time, catalyst dosage, molar ratio of *n*-octanol to glucose on the conversion rate of glucose were systematically investigated. In addition, the regeneration and recyclability of SO_3H-functionalized ILs were also evaluated. Finally, the catalytic mechanism of SO_3H-functionalized ILs was further studied in detail by molecular simulation.

2 Experimental section

2.1 Materials

Sulfuric acid, toluene, ethyl acetate, pyridine, *p*-nitroaniline, glucose and *n*-octanol, monopotassium monosodium tartrate tetrahydrate, methylene blue were purchased from Beijing Chemical Company and were of analytical grade. *N*-Methylimidazole, copper(II) sulfate pentahydrate were purchased from Sinopharm Chemical Reagent Co., Ltd. 1,3-Propanesulfonate was purchased from Aladdin Industrial Corporation. *p*-Toluenesulfonic acid monohydrate was purchased from Tokyo Chemical Industry Co., Ltd. Ultrapure water was obtained by the water purification system (Milli-Q Direct-8). All reagents were commercially available and used as received without further purification.

2.2 Synthesis of SO_3H-functionalized ILs

The SFILs including 1-(3-sulfonic)-propyl-3-methyl imidazolium hydrosulfate ([PSmim][HSO_4]), 1-(3-sulfonic)-propyl-3-methyl imidazolium *p*-toluenesulfonate ([PSmim][*p*TSA]), 1-(3-sulfonic)-propyl pyridine hydrosulfate ([PSPy][HSO_4]) and 1-(3-sulfonic)-propyl pyridine *p*-toluenesulfonate ([PSPy][*p*TSA]) were synthesized according to the literatures.[20,24] *N*-Methylimidazole (0.22 mol) and 1,3-propane sultone (0.22 mol) were dissolved in toluene (60 mL) as an inert solvent, which were added to a round-bottomed flask (200 mL) fitted with a reflux condenser and stirred at 343.15 K, 353.15 K, 363.15 K, 373.15 K for 24 h under a nitrogen atmosphere. Afterwards, the white precipitates were filtered off and washed several times with ethyl acetate to get 1-(3-sulfonic)-propyl-3-methyl imidazolium (PSmim), which was monitored by copper(II) chloride in ethanol and no blue colour could be found. Then, PSmim was dried in a vacuum under 343.15 K for 48 h. [PSmim][HSO_4] was obtained by a dropwise addition of one equivalent of concentrated sulfuric acid (98%) through constant pressure funnel to an aqueous solution of PSmim that the mixture was stirred at 353.15 K for 12 h. Finally, the water of mixture was removed by a rotary evaporator, and then light yellow viscous [PSmim][HSO_4] was obtained. [PSmim][HSO_4] was dried under vacuum at 343.15 K for 48 h and stored in a desiccator. Other SFILs [PSmim][*p*TSA], [PSPy][HSO_4] and [PSPy][*p*TSA] were prepared according to a procedure similar to that used for [PSmim][HSO_4]. All these SFILs were dried under vacuum at 343.15 K for 48 h before usage and the water contents were all below 800 ppm measured by Karl Fischer Coulometers C20.

2.3 Characterization and physicochemical properties of SFILs

^{1}H NMR spectra were recorded on a Bruker spectrometer (600 Hz) in deuterium oxide (D_2O). The Fourier transform infrared-spectra (FTIR) were obtained in the range of 400–4000 cm^{-1} on a Thermo Nicolet 380 spectrometer. Electrospray ionization mass spectrometry (ESI-MS) were obtained in both positive and negative modes with a Bruker micrOTOF-Q II. The ^{1}H NMR, FTIR and ESI-MS data are given in the ESI.†

The determination of four SFILs decomposition temperatures were measured on thermogravimetric analysis (TGA Q5000 V3.15 Build 263) by heating sample from room temperature to 873.15 K at a heating rate of 10 K min^{-1} under the flow 25 mL min^{-1} of nitrogen atmosphere. The decomposition temperatures of four SFILs are all above 473.15 K and shown in ESI,† which means that these four SFILs show excellent thermodynamic stability and suitable for glycosidation as catalysts.

2.4 The acidities evaluation of SFILs

The Brønsted acidities associated with the Hammett acidity function of four SFILs were measured in aqueous solutions. *p*-Nitroaniline was chosen as the indicator for the measurement of the Hammett acidity function through UV-Vis (UV-2550, Shimadzu) spectroscopy.[25–27] Therefore, the Hammett acidities function (H_0) of four SFILs could be calculated *via* the following equation:

$$H_0 = pK_a(InH^+) + \log([In]/[InH^+]) \quad (1)$$

Table 1 The acidities of four SFILs

SFIL	Absorbance [AU]	[In]/(%)	[InH^+]/(%)	H_0
p-Nitroaniline[a]	0.132	100	0	
[PSmim][HSO_4]	0.088	66.7	33.3	1.29
[PSPy][HSO_4]	0.091	68.9	31.1	1.34
[PSmim][*p*TSA]	0.099	75.0	25.0	1.47
[PSPy][*p*TSA]	0.101	76.5	23.5	1.50

[a] Indicator: *p*-nitroaniline: 0.01 mmol L^{-1}, SFIL: 0.125 mmol L^{-1}.

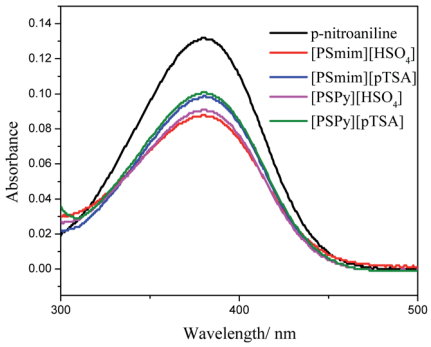

Fig. 3 Absorbance spectra of 4-nitroaniline for four SFILs in ultrapure water.

where, $pK_a(InH^+)$ is the pK_a value of the protonated *p*-nitroaniline indicator in aqueous solution (0.99), and [In] and [InH^+] are the molar percent of the unprotonated and protonated forms of the indicator, respectively. The UV/Vis spectra of both unprotonated and protonated forms of the indicator showed a specific absorption at about 380 nm in aqueous solution of *p*-nitroaniline and the results are displayed in the Table 1 and Fig. 3. It could be seen that the characteristic absorption peak decreased as the acidity of the solution increased and the acidities (H_0) of four SFILs were calculated and following the order: [PSmim][HSO_4] ($H_0 = 1.29$) < [PSPy][HSO_4] ($H_0 = 1.34$) < [PSmim][*p*TSA] ($H_0 = 1.47$) < [PSPy][*p*TSA] ($H_0 = 1.50$). It is exhibited that [PSmim][HSO_4] is the most acidic SFIL among four SFILs.

2.5 Glucosidation reaction

In the synthesis process of APG, a mixture of the glucose, *n*-octanol, and SO_3H-functionalized ILs were added to a round bottom flask (100 mL) fitted with a reflux condenser that was connected to Schlenk line and reacted at desired temperature for certain time. After the reaction finished, the mixture was cooled down to room temperature. Then, the yields of glycosides were determined by Fehling reagent.

3 Results and discussion

3.1 Screening of SFILs catalysts for glycosylation

On account of Fischer's glycosylation reaction model, four SFILs as catalysts were used for the direct glycosylation. The catalytic activities of four SFILs were evaluated according to the results of conversion rate of glucose under the same experiment condition and the results are shown in Table 2. It can be seen that [PSmim][HSO_4] exhibited the best catalytic performance for glucose conversion at the conditions of 353.15 K, 24 h. Obviously, the results also indicated that the conversion rate of glucose with four SFILs decreased following the order [PSmim][HSO_4] > [PSPy][HSO_4] > [PSmim][*p*TSA] > [PSPy][*p*TSA], which has a similar trend in the synthesis of furylmethane and esterification.[22,28] Moreover, the acidities (H_0) of four SFILs follow the order: [PSmim][HSO_4] ($H_0 = 1.29$) < [PSPy][HSO_4] ($H_0 = 1.34$) < [PSmim][*p*TSA] ($H_0 = 1.47$) < [PSPy][*p*TSA] ($H_0 = 1.50$), which has a similar sequence of catalytic activity in the APG synthesis. Xing *et al.* also found that the acidity of [PSPy][HSO_4] is stronger than that of [PSPy][*p*TSA], which is consistent with the activity order of [PSPy][HSO_4] and [PSPy][*p*TSA] in the synthesis of D,L-α-tocopherol as catalyst.[21] Therefore, the difference of acidities of four SFILs may be the reason of remarkable difference in conversion of glucose. In addition, the conversion of glycose for [PSmim][HSO_4] reached up to 92.8%, which is higher than that reported by Jacques Augé *et al.* For their research, the conversion of glycose is 74% when 1-butyl-3-methylimidazolium trifluoromethanesulfonate ([Bmim][OTf]) was used as catalyst for APG synthesis.[6] The yield of APG is only 16% when the KSF/O as catalyst, which was investigated by Sandrine Brochette *et al.*[29] These results indicated that these SFILs have good catalytic performance. Due to the highest catalytic activity of [PSmim][HSO_4] for glucosylation, the [PSmim][HSO_4] was investigated as a typical example in the subsequent work. Furthermore, in order to optimize experiment conditions, reaction temperature, reaction time, catalyst dosage, molar ratio of *n*-octanol to glucose as well as the recycle of catalyst were investigated systematically. What's more, the reaction mechanism of APG synthesis using SFILs as catalysts were investigated further by molecular simulation.

3.2 Effect of the reaction temperature

The direct glycosylation was carried out at different temperature ranging from 343.15 K to 373.15 K. The results of the conversion rate of glucose are shown in Table 3. It could be seen that the reaction temperature had a significant influence on the catalytic performance. When the reaction temperature increased from 343.15 K to 353.15 K, the conversion rate of glucose increased sharply from 57.6% to 90.1%. However, when the reaction temperature increased from 353.15 K to 373.15 K, the

Table 2 SFILs screening[a]

SFIL	Conversion of glycose[b]/%
[PSmim][HSO_4]	92.8
[PSPy][HSO_4]	83.4
[PSmim][*p*TSA]	82.5
[PSPy][*p*TSA]	81.5

[a] Reaction conditions: glucose (0.018 mol), *n*-octanol (5 equiv.), catalyst (0.05 equiv.), reaction temperature (353.15 K), reaction time (24 h). [b] The conversion of glycose was measured using Fehling reagent.

Table 3 The effect of temperature on glucosylation[a]

Temperature/K	Conversion of glycose[b]/%
343.15	57.6
353.15	92.8
363.15	88.8
373.15	84.8

[a] Reaction conditions: glucose (0.018 mol), *n*-octanol (5 equiv.), [PSmim][HSO_4] (0.05 equiv.), reaction time (24 h). [b] The conversion of glycose was measured using Fehling reagent.

Table 4 The effect of reaction time on glucosylation[a]

Reaction time/h	Conversion of glycose[b]/%
2	73.8
4	79.3
6	86.1
8	90.1
12	90.7
24	92.8

[a] Reaction conditions: glucose (0.018 mol), *n*-octanol (5 equiv.), [PSmim][HSO_4] (0.05 equiv.), reaction temperature (353.15 K). [b] The conversion of glycose was measured using Fehling reagent.

conversion rate of glucose decreased slightly from 90.1% to 84.8%. It is obvious that the glycosylation is a dynamic equilibrium reaction. Within the given time, the reaction rate was accelerated and the high conversion rate of glucose could be obtained with the increasement of temperature. On the other hand, the high temperature will lead to the degradation of glucosylation, which had been confirmed by Ludot *et al.*[5] According to the conversion rate of glucose, the temperature of 353.15 K was chosen as the optimal reaction temperature.

3.3 Effect of the reaction time

For a chemical reaction, the reaction time usually play an important role in determining the conversion rate of reactants. Therefore, the conversion rate of glucose at different reaction time was studied systematically using [PSmim][HSO_4] as catalyst at 353.15 K. As seen from Table 4, when the reaction time increased from 2 h to 24 h, the conversion rate of glucose increased greatly from 73.8% to 92.8%. It is indicated that the reaction equilibrium did not reach until the reaction time was up to 8 h. As the reaction time increased from 8 h to 24 h, the conversion rate of glucose increased slightly. Therefore, the proper reaction time was set at 8 h, which was less than 24 h reported by Augé *et al.*[6]

3.4 Effect of the catalyst dosage

To study the effect of the catalyst dosage on the conversion rate of glucose, the direct glucosylation of *n*-octanol with glucose was carried out at the same conditions of glucose (0.018 mol), *n*-octanol (5 equiv.), temperature (353.15 K), time (8 h) and the results were displayed in Table 5. It can be seen that the conversion rate of glucose increased significantly from 55.9% to 85.2% with the increase of catalyst dosage from 2 mol% to 3 mol%. The increasing trend of conversion rate of glucose became slower when the catalyst dosage was up to 5 mol%. Furthermore, the increase of catalyst dosage had slight influence on the conversion rate of glucose when the amount of catalyst was above 5 mol%. Therefore, the optimal catalyst dosage was 5 mol% in this study.

Table 5 The effect of catalyst dosage on glucosylation using [PSmim][HSO_4] as catalyst

Catalyst dosage/%	Conversion of glycose/%
2	55.9
3	85.2
4	87.8
5	90.1
7	90.2

3.5 Effect of *N*-octanol and glucose molar ratio

In the reported research, the molar ratio of long tail fatty alcohols to glucose should exceed 5 : 1 for the glucosylation due to low catalytic activity of the catalysts.[2] In this work, the effect of *n*-octanol and glucose molar ratio for the glucosylation on the conversion rate of glucose was investigated at the same conditions. As shown in Table 6, when the molar ratio of *n*-octanol to glucose increased from 1 : 1 to 5 : 1, the conversion rate of glucose increased from 76.8% to 90.1%. It is exhibited that [PSmim][HSO_4] shown a stable catalytic performance when the molar ratio of *n*-octanol to glucose decreased from 5 : 1 to 3 : 1, which indicated that the reactor volume could be decreased to some extent. Camille Ludot synthesized APG using cyclic sulfolane with the yield up to 83%, but excess long chain alcohol needs to be added (450 times the amount of glucose).[5] This also demonstrated that [PSmim][HSO_4] has better catalytic performance than traditional catalyst.

3.6 Recycling of the ionic liquid catalyst

For the industrial application of catalysts, the regeneration and subsequent recycling of catalysts are of vital importance. The recyclability of the [PSmim][HSO_4] as catalyst for direct glucosylation was carried out under the optimization conditions of glucose (0.018 mol), *n*-octanol (5 equiv.), [PSmim][HSO_4] (0.05 equiv.), temperature (353.15 K), time (8 h). The [PSmim][HSO_4] is nearly insoluble in ethylacetate, while *n*-octanol and glucosylation product are miscible with ethylacetate. When the glucosylation reaction finished, the product is divided into two phases after the addition of ethylacetate. The upper layer is a mixture of ethylacetate, excess *n*-octanol and APG, and [PSmim][HSO_4] and few glucose are present in the under layer. APG can be separated from the upper mixture by rectification

Table 6 The effect of octanol and glucose molar ratio on glucosylation[a]

N-Octanol and glucose molar ratio	Conversion of glycose[b]/%
1 : 1	76.8
2 : 1	79.3
3 : 1	87.5
4 : 1	88.1
5 : 1	90.1

[a] Reaction conditions: glucose (0.018 mol), [PSmim][HSO_4] (0.05 equiv.), reaction temperature (353.15 K), reaction time (8 h). [b] The conversion of glycose was measured using Fehling reagent.

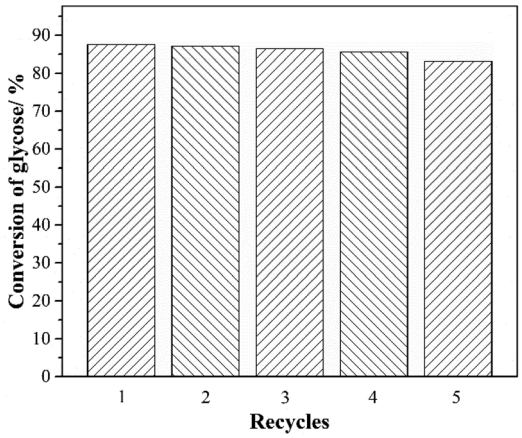

Fig. 4 Recycling use of [PSmim][HSO_4] as catalyst for glucosylation. Reaction conditions: glucose (0.018 mol), *n*-octanol (3 equiv.), catalyst (0.05 equiv.), reaction temperature (353.15 K), reaction time (8 h).

and re-extraction. What's more, the [PSmim][HSO_4] of under layer can be reused without further treatment. The [PSmim][HSO_4] was reused consecutively in 5 recycles without purification further and the performance of catalyst exhibited slightly decrease from 88.2% to 83.2% (Fig. 4). It is indicated that [PSmim][HSO_4] displayed great stability and reusability as catalyst for direct glucosylation.

3.7 Mechanism analysis

To reveal the catalytic mechanism of glucosylation with SFILs as catalyst, the molecular simulation was used to investigate the role of SFILs in the synthesis of APG, which take [PSmim][HSO_4] as an example. All the geometries optimized were carried out in the M06-2X-D3/6-311+G** with Gaussian 09 software.[30–32] The protonated position of glucose was determined by the interaction energy. The interaction energy were measured when $[HSO_4]^-$ bind to the different hydroxyl on glucose (named O1, O2, O3, O4, O6, respectively, and O1′, O2′, O3′ were oxygen on hydrogen sulfate). The results of interaction positions (interaction energy) were displayed in Fig. 5 and Table 7. From the results of interaction energy, protonated hydroxyl had

Table 7 The related parameters of hydrogen between oxygen on the hydroxyl of glucose and hydrogen sulfate

Structure	H-bond	ΔE (kJ mol^{-1})
(b)	O1···H–O1′ O2–H···O2′	−145.51
(c)	O2···H–O1′ O3–H···O2′	−109.47
(d)	O6–H···O3′ O4–H···O2′ O3···H–O1′	−118.44
(e)	O4–H···O2′ O4···H–O1′	−88.82
(f)	O6···H–O1′ O4–H···O2′	−89.44

a sequence as follows: O1 > O3 > O2 > O6 > O4, which indicated that O1 was the position that was most preferentially of glucose by [PSmim][HSO_4].[33] In addition, the bonds length of O1–H···O1′ (2.10 Å) and O2–H···O2′ (1.69 Å) were shorter than the van der Waals (2.72 Å),[34] implying there are hydrogen bonds between hydrogen sulfate and glucose. The presence of hydrogen bonds makes glucose more reactive.[21,35,36] Therefore, O1 position of glucose was easier protonated by [PSmim][HSO_4].

The interaction energy (ΔE) is defined as the energy difference between the conformer (E_{ab}, the energy of the structure in the combined state of AB) and the corresponding isolated ions (E_a, E_b, the energy of the structure when A and B are optimized separately):

$$\Delta E = 2625.5 \times [E_{ab} - E_a - E_b], \text{ kJ mol}^{-1} \quad (2)$$

On the other hand, in order to further investigate the reaction mechanism between the *n*-octanol and protonated glucose, the changes of the electronegativity changes of oxygen of *n*-octanol and the bond lengths changes of hydroxyl of *n*-octanol before and after reaction were simulated by Gaussian. The atomic charges were calculated by the natural bond orbital (NBO) method.[37,38] The bond length of hydroxyl and NBO charge of the oxygen of hydroxyl in *n*-octanol were plotted in Fig. 6, which showed that [PSmim][HSO_4] had an influence on the bond length and charge density of the hydroxyl of *n*-octanol.

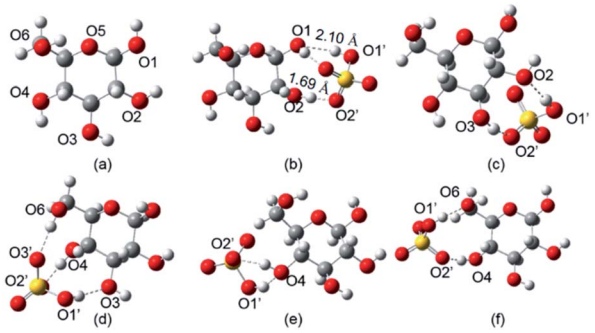

Fig. 5 The optimal structure of glucose was protonated hydrogen sulfate in the position of O1, O2, O3, O4, O6 (S, yellow; O, red; C, gray; H, white).

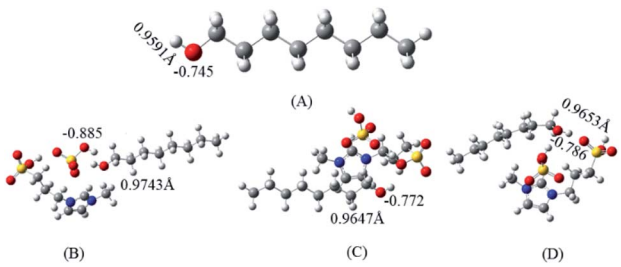

Fig. 6 The influence to the NBO charge of the oxygen on the hydroxyl and the bond length of hydroxyl in the process of *n*-octanol binding to glucose by [PSmim][HSO_4] (N, blue; S, yellow; O, red; C, gray; H, white). (A) *n*-octanol, (B–D) the optimal interaction structure between glucose and [PSmim][HSO_4].

The electronegativity of the oxygen of hydroxyl in *n*-octanol (B–D) and their original were −0.825, −0.772, −0.786, and −0.745, respectively, which indicated the nucleophilicity of the oxygen were stronger and the hydroxyl would bind to protonated glucose easier because of the appearance of [PSmim][HSO_4]. In addition, the O–H bond length of the hydroxyl of *n*-octanol (B 0.9743 Å, C 0.9647 Å, D 0.9653 Å) became longer than initial condition (A 0.9591 Å), implying the oxyhydrogen bond of *n*-octanol would break off easier on account of the appearance of [PSmim][HSO_4]. Moreover, the presence of hydrogen bonds between SFILs and *n*-octanol would promote removal of hydrogen ion from *n*-octanol more readily, which may be one of the reasons for the high catalytic activity of SFILs. What's more, the results of the bond lengths changes of hydroxyl haves a better agreement with the results of the electronegativity changes of oxygen. Therefore, owning to the appearance of [PSmim][HSO_4], it had an acceleration effect on the reaction process of *n*-octanol and protonated glucose, which may be one of the reason of high glucose conversion rate in the synthesis of APG.

4 Conclusions

In summary, four thermostable SFILs were synthesized and used as catalysts for direct glucosylation. According to the results, [PSmim][HSO_4] displayed the highest conversion of glucose (92.8%) than other three SFILs. Furthermore, the reaction time could be shortened from 24 h to 8 h and the molar ratio of *n*-octanol to glucose was decreased to 3 : 1. In addition, [PSmim][HSO_4] exhibited excellent recycle performance without significant decrease of conversion of glycose after five recycles. The catalytic activity of SFILs was dependent on their anion and the catalytic activity could be enhanced *via* the increase of the anion's Brønsted acidity, which had a great agreement with the experimental results. Moreover, it was demonstrated that SFILs would proton glucose easier and *n*-octanol would remove hydrogen ion from hydroxyl more readily due to the formation of hydrogen bond by molecular simulation. Taking aforementioned performance into consideration, [PSmim][HSO_4] might be used as a promising catalyst for APG synthesis.

Conflicts of interest

There are no conflicts to declare.

Acknowledgements

We are grateful to the National Natural Science Foundation of China (No. 22078323, 51574215, 21436010).

Notes and references

1 C. Marinkovic and B. Estrine, *Green Chem.*, 2010, **12**, 1929–1932.
2 W. von Rybinski and K. Hill, *Angew. Chem., Int. Ed.*, 1998, **37**, 1328–1345.
3 S. Iglauer, Y. Wu, P. Shuler, Y. Tang and W. A. Goddard, *Colloids Surf., A*, 2009, **339**, 48–59.
4 M. M. A. El-Sukkary, N. A. Syed, I. Aiad and W. I. M. El-Azab, *J. Surfactants Deterg.*, 2008, **11**, 129–137.
5 C. Ludot, B. Estrine, J. Le Bras, N. Hoffmann, S. Marinkovic and J. Muzart, *Green Chem.*, 2013, **15**, 3027–3030.
6 J. Augé and G. Sizun, *Green Chem.*, 2009, **11**, 1179–1183.
7 N. Villandier and A. Corma, *Chem. Commun.*, 2010, **46**, 4408–4410.
8 D. Mishra and V. K. Sinha, *Int. J. Adhes. Adhes.*, 2010, **30**, 47–54.
9 W. Deng, M. Liu, Q. Zhang, X. Tan and Y. Wang, *Chem. Commun.*, 2010, **46**, 2668–2670.
10 D. S. von Es, S. Marinkovic, X. Oduber and B. Estrine, *J. Surfactants Deterg.*, 2013, **16**, 147–154.
11 B. Kai and F. T. Lutz, *Fett/Lipid*, 1998, **100**, 36–41.
12 A. S. Amarasekara, *Chem. Rev.*, 2016, **116**, 6133–6183.
13 X. L. Meng, Y. Nie, J. Sun, W. G. Cheng, J. Q. Wang, H. Y. He and S. J. Zhang, *Green Chem.*, 2014, **16**, 2771–2778.
14 S. Wang, Y. Zhao, H. Lin, J. Chen, L. Zhu and Z. Luo, *Green Chem.*, 2017, **19**, 3869–3879.
15 A. A. Chaugule, A. H. Tamboli and H. Kim, *Fuel*, 2017, **200**, 316–332.
16 P. Wang, X. Chen, D. L. Wang, Y. Q. Li and Y. Liu, *Green Energy Environ.*, 2017, **2**, 419–427.
17 T. L. Greaves and C. J. Drummond, *Chem. Rev.*, 2015, **115**, 11379–11448.
18 P. Sarma, A. K. Dutta and R. Borah, *Catal. Surv. Asia*, 2017, **21**, 70–93.
19 A. C. Cole, J. L. Jensen, I. Ntai, K. L. T. Tran, K. J. Weaver, D. C. Forbes and J. H. Davis, *J. Am. Chem. Soc.*, 2002, **124**, 5962–5963.
20 Y. Leng, J. Wang, D. Zhu, X. Ren, H. Ge and L. Shen, *Angew. Chem., Int. Ed.*, 2009, **48**, 168–171.
21 H. Xing, T. Wang, Z. Zhou and Y. Dai, *J. Mol. Catal. A: Chem.*, 2007, **264**, 53–59.
22 S. H. Shinde and C. V. Rode, *Green Chem.*, 2017, **19**, 4804–4810.
23 H. Li, S. Yu, F. Liu, C. Xie and L. Li, *Catal. Commun.*, 2007, **8**, 1759–1762.
24 H. Xing, T. Wang, Z. Zhou and Y. Dai, *Ind. Eng. Chem. Res.*, 2005, **44**, 4147–4150.
25 C. Thomazeau, H. O. Bourbigou, L. Magna, S. Luts and B. Gilbert, *J. Am. Chem. Soc.*, 2003, **125**, 5264–5265.
26 L. Shen, H. Yin, A. Wang, X. Lu, C. Zhang, F. Chen, Y. Wang and H. Chen, *J. Ind. Eng. Chem.*, 2014, **20**, 759–766.
27 L. Zhang, L. He, C. B. Hong, S. Qin and G. H. Tao, *Green Chem.*, 2015, **17**, 5154–5163.
28 J. Gui, X. Cong, D. Liu, X. Zhang, Z. Hu and Z. Sun, *Catal. Commun.*, 2004, **5**, 473–477.
29 S. Brochette, G. Descotes, A. Bouchu, Y. Queneau, N. Monnier and C. Petrier, *J. Mol. Catal. A: Chem.*, 1997, **123**, 123–130.
30 M. J. Frisch, G. W. Trucks, H. B. Schlegel, G. E. Scuseria, M. A. Robb, J. R. Cheeseman, G. Scalmani, V. Barone, G. A. Petersson, H. Nakatsuji, X. Li, M. Caricato, A. Marenich, J. Bloino, B. G. Janesko, R. Gomperts,

B. Mennucci, H. P. Hratchian, J. V. Ortiz, A. F. Izmaylov, J. L. Sonnenberg, D. Williams-Young, F. Ding, F. Lipparini, F. Egidi, J. Goings, B. Peng, A. Petrone, T. Henderson, D. Ranasinghe, V. G. Zakrzewski, J. Gao, N. Rega, G. Zheng, W. Liang, M. Hada, M. Ehara, K. Toyota, R. Fukuda, J. Hasegawa, M. Ishida, T. Nakajima, Y. Honda, O. Kitao, H. Nakai, T. Vreven, K. Throssell, J. A. Montgomery, J. E. Peralta Jr, F. Ogliaro, M. Bearpark, J. J. Heyd, E. Brothers, K. N. Kudin, V. N. Staroverov, T. Keith, R. Kobayashi, J. Normand, K. Raghavachari, A. Rendell, J. C. Burant, S. S. Iyengar, J. Tomasi, M. Cossi, J. M. Millam, M. Klene, C. Adamo, R. Cammi, J. W. Ochterski, R. L. Martin, K. Morokuma, O. Farkas, J. B. Foresman and D. J. Fox, *Gaussian 09*, Gaussian, Inc., Wallingford, CT, 2009.

31 Y. Zhao and D. G. Truhlar, *Theor. Chem. Acc.*, 2007, **120**, 215–241.

32 S. Grimme and M. Steinmetz, *Phys. Chem. Chem. Phys.*, 2013, **15**, 16031–16042.

33 Q. Wang, X. Yao, S. Tang, X. Lu, X. Zhang and S. Zhang, *Green Chem.*, 2012, **14**, 2559–2566.

34 A. Bondi, *J. Phys. Chem.*, 1964, **68**, 441–451.

35 S. Zhang, X. Qi, X. Ma, L. Lu and Y. Deng, *J. Phys. Chem. B*, 2010, **114**, 3912–3920.

36 I. W. Kim, M. D. Jang, Y. K. Ryu, E. H. Cho, Y. K. Lee and J. H. Park, *Anal. Sci.*, 2002, **18**, 1357–1360.

37 J. K. Badenhoop and F. Weinhold, *J. Chem. Phys.*, 1997, **107**, 5406–5421.

38 T. Lu and F. Chen, *J. Theor. Comput. Chem.*, 2012, **11**, 163–183.